Progress In Electromagnetics Research C, Vol. 128, 29–37, 2023

Scattering of a Gaussian Beam Wave by Multiple Homogeneous Anisotropic Cylinders

Shi-Chun Mao[1, *], Hai-Ying Li[2], Juan Cao[1], and Fei Chen[1]

Abstract—Electromagnetic scattering of a Gaussian beam wave from an array of parallel homogeneous anisotropic cylinders is presented. The transmitted fields in the anisotropic cylinders are expressed as an infinite summation of eigen-plane waves with different polar angles. The expression of the Gaussian beam is represented as a product of a well-known scattering of a plane wave and a weighting function. The incident field is expressed in local cylindrical coordinates and the scattered field is the summation of contribution of all cylinders. Using the addition theorem of Hankel function, the expression of the scattered field can be transformed from local coordinates to others. By enforcing the boundary conditions on the surface of each cylinder, an infinite set of equations is obtained which can be written in a matrix form. Scattering cross sections and near fields are analyzed and compared finally.

1. INTRODUCTION

Cylindrical structures have long been the subject of extensive investigation since a great variety of practical scatterers can be modeled by a suitable arrangement of cylinders [1–3]. Electromagnetic scattering by multiple cylinders has been discussed in the past 20 years [4–7]. For example, a formulation for multiple scattering by dielectric or metamaterial conducting cylinders has been presented by Shooshtari and Sebak [8]. However, in many practical applications and some experimental requirements, a bounded incident beam instead of an infinitely extended plane wave is utilized.

The two-dimensional scattering of a Gaussian beam wave by multiple homogeneous anisotropic cylinders is characterized in this paper. Firstly, the transmitted fields in the anisotropic cylinders are expressed as an infinite summation of eigen-plane waves with different polar angles in their local coordinates. Secondly, the expression of the Gaussian beam is represented as a product of a well-known scattering of a plane wave and a weighting function. Thirdly, the analytical formulation of multiple homogeneous anisotropic cylinders is developed. Finally, numerical results are demonstrated to show the behavior of scattering electromagnetic waves by homogeneous anisotropic cylinders. The case of incident TE wave is analyzed in detail, and that of TM wave is outlined. The time dependence is assumed to be $\exp(j\omega t)$ throughout the paper.

2. FORMULATION

The cross-section geometry of M homogeneous anisotropic circular cylinders is shown in Fig. 1, and the cylinders radii denoted by $a_i\,(i = 1, 2, \ldots, M)$ and their local coordinates are fixed at origins

Received 4 October 2022, Accepted 20 December 2022, Scheduled 24 December 2022

* Corresponding author: Shi-Chun Mao (mscgroup@163.com).

[1] Institute of Information Engineering, Suqian University, Suqian, Jiangsu 223800, China. [2] School of Physics, Xidian University, Xi'an, Shaanxi 710071, China.

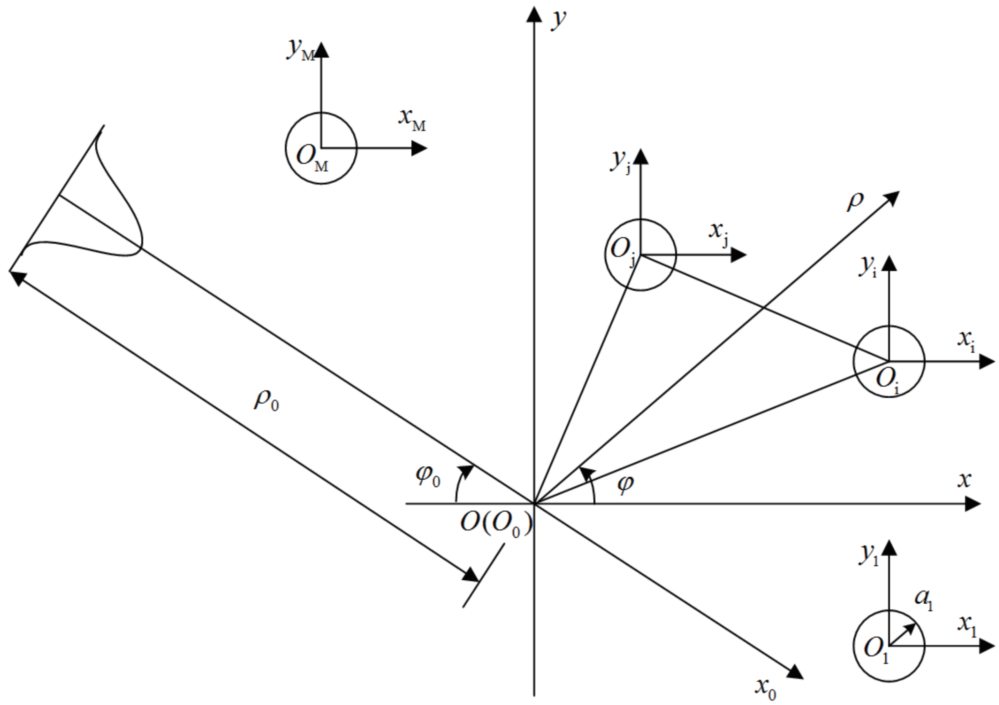

Figure 1. Geometry of the problem.

O_i $(i = 1, 2, \ldots, M)$ as shown in the figure. The homogeneous anisotropic cylinders are characterized by the following permittivity and permeability tensors in their local coordinates:

$$\bar{\bar{\varepsilon}}_i = \begin{bmatrix} \varepsilon_{x_ix_i} & \varepsilon_{x_iy_i} & 0 \\ \varepsilon_{y_ix_i} & \varepsilon_{y_iy_i} & 0 \\ 0 & 0 & \varepsilon_{z_iz_i} \end{bmatrix}, \quad \bar{\bar{\mu}}_i = \begin{bmatrix} \mu_{x_ix_i} & \mu_{x_iy_i} & 0 \\ \mu_{y_ix_i} & \mu_{y_iy_i} & 0 \\ 0 & 0 & \mu_{z_iz_i} \end{bmatrix}. \tag{1}$$

2.1. Expression of Transmitted Wave

The magnetic fields in the anisotropic cylinders can be expressed as an infinite summation of eigen-plane waves with different polar angles in their local coordinates [9],

$$H_z^c(\rho_i, \varphi_i) = \sum_{n=-\infty}^{\infty} j^{-n} e^{jn\varphi_i} \sum_{m=-\infty}^{\infty} C_{im} H_{nm}(\rho_i) \quad (i = 1, 2, \ldots, M.), \quad (\rho_i \leq a_i) \tag{2}$$

where

$$H_{nm}(\rho_i) = \int_0^{2\pi} J_n(k_i(\xi)\rho_i) e^{j(m-n)\xi} d\xi, \quad \gamma_i = \varepsilon_{x_ix_i}\varepsilon_{y_iy_i} - \varepsilon_{x_iy_i}\varepsilon_{y_ix_i}, \tag{3}$$

$$k_i(\xi) = \sqrt{\frac{\omega^2 \mu_{z_iz_i} \gamma_i}{\varepsilon_{i+} + \varepsilon_{i-} \cos 2\xi + \sigma_{i+} \sin 2\xi}}, \quad \varepsilon_{i\pm} = \frac{1}{2}(\varepsilon_{x_ix_i} \pm \varepsilon_{y_iy_i}), \quad \sigma_{i\pm} = \frac{1}{2}(\varepsilon_{x_iy_i} \pm \varepsilon_{y_ix_i}). \tag{4}$$

C_{im} are unknown coefficients, and $J_n(k_i\rho)$ is the Bessel function of the first kind and order n.

2.2. Incident and Scattered Waves

A Gaussian beam source located at $(x_0 = -\rho_0,\ y_0 = 0)$ is incident to the global coordinate origin, making an angle φ_0 clockwise with respect to the negative x-axis.

Let us consider the case where a beam source, e.g., horn antenna, is located at $x_0 = -\rho_0$ as illustrated in Fig. 1. The z-component of magnetic field of the incident Gaussian beam source is expressed as

$$H_z^{inc}(x_0 = -\rho_0, y_0) = H_0 e^{-\beta^2 y_0^2}, \tag{5}$$

where

$$\beta^2 = a_0^2 + jb_0^2 \tag{6}$$

and $1/|\beta|$ corresponds to the beamwidth of the incident wave.

The z-component of the magnetic field from the source can be approximately expanded in terms of cylindrical harmonic functions in global coordinate as follows [10]:

$$H_z^{inc}(\rho, \varphi) = \sum_{n=-\infty}^{\infty} A_n j^{-n} J_n(k\rho) e^{jn(\varphi+\varphi_0)} \tag{7}$$

where

$$A_n = \frac{e^{-jk\rho_0}}{\sqrt{1-jZ_0}} e^{-\left(\frac{n\beta}{k}\right)^2 \frac{1}{1-jZ_0}} \left[1-2\left(\frac{\beta}{k\sqrt{1-jZ_0}}\right)^4 n^2 + \frac{4}{3}\left(\frac{\beta}{k\sqrt{1-jZ_0}}\right)^6 n^4 + \ldots\right], \quad Z_0 = \frac{2\beta^2\rho_0}{k}. \tag{8}$$

k is the free space wavenumber. This expression is valid for $|(\beta\lambda)^2| < 0.3$ and $b/\lambda < 5.0$.

Further, the incident field can be expressed in local coordinate systems of the i-th cylinder (ρ_i, φ_i), $(i = 1, 2, \ldots, M.)$, whose center is located at (ρ_i', φ_i') $(i = 1, 2, \ldots, M.)$ in global coordinate,

$$H_z^{inc}(\rho_i, \varphi_i) = e^{-jk\rho_i' \cos(\varphi_i'+\varphi_0)} \sum_{n=-\infty}^{\infty} A_n j^{-n} J_n(k\rho_i) e^{jn(\varphi_i+\varphi_0)} \tag{9}$$

Similarly, the scattered field is the summation of contribution of all M cylinders and can be expressed as

$$H_z^s(\rho_l, \varphi_l) = \sum_{l=1}^{M} \sum_{m=-\infty}^{\infty} B_{lm} j^{-m} H_m^{(2)}(k\rho_l) \exp(jm\varphi_l), \quad (\rho_l > a_l, l = 1, 2, \ldots, M.) \tag{10}$$

where B_{lm} are unknown coefficients, and $H_n^{(2)}$ is the Hankel function of the second kind.

2.3. Boundary Conditions

The tangential component of the electric field in cylinders $(\rho_i \le a_i)$ can be expressed in local coordinates as follows

$$j\omega\gamma E_{\varphi_i}^c(\rho_i, \varphi_i) = -\left[\varepsilon_{\rho_i\rho_i}(\varphi_i)\frac{\partial H_z^c}{\partial \rho_i} + \varepsilon_{\varphi_i\rho_i}(\varphi_i)\frac{1}{\rho_i}\frac{\partial H_z^c}{\partial \varphi_i}\right], \quad (\rho_i \le a_i), \tag{11}$$

which can be expressed as

$$E_{\varphi_i}^c(\rho_i, \varphi_i) = \sum_{n=-\infty}^{\infty} j^{-n} e^{jn\varphi_i} \sum_{m=-\infty}^{\infty} C_{im} E_{nm}(\rho_i), \quad (\rho_i \le a_i), \tag{12}$$

where

$$E_{nm}(\rho_i) = \int_0^{2\pi} \frac{k(\xi)}{\omega\gamma_i}\left[j\varepsilon_{\rho_i\rho_i}(\xi) J_n'(k(\xi)\rho_i) - \frac{n\varepsilon_{\varphi_i\rho_i}(\xi+\pi/2)}{k(\xi)\rho_i} J_n(k(\xi)\rho_i)\right] e^{j(m-n)\xi} d\xi, \tag{13}$$

While taking into account that in the vacuum or isotropic media, the tangential component of the electric field can be written as

$$E_{\varphi_i}^{inc(s)} = \frac{j}{\omega\varepsilon_0}\frac{\partial H_z^{inc(s)}}{\partial \rho_i}, \quad (\rho_i > a_i), \tag{14}$$

where,

$$E_{\varphi_i}^{inc}(\rho_i,\varphi_i) = j\sqrt{\frac{\mu_0}{\varepsilon_0}}e^{jk\rho_i'\cos(\varphi_i'+\varphi_0)}\sum_{n=-\infty}^{\infty}A_n j^{-n}J_n'(k\rho)e^{jn(\varphi_i+\varphi_0)}, \quad (\rho_i > a_i) \tag{15}$$

$$E_{\varphi_l}^{s}(\rho_l,\theta_l) = j\sqrt{\frac{\mu_0}{\varepsilon_0}}\sum_{l=1}^{M}\sum_{m=-\infty}^{\infty}B_{lm}j^{-m}H_m^{(2)'}(k\rho_l)e^{jn\varphi_l}. \quad (\rho_l > a_l) \tag{16}$$

The tangential components of the electric and magnetic fields are continuous on the interface between anisotropic cylinder and free space, and the boundary conditions can be expressed as

$$H_z^c = H_z^{inc} + H_z^s, \quad (\rho_i = a_i) \tag{17}$$

$$E_{\varphi_i}^c = E_{\varphi_i}^{inc} + E_{\varphi_i}^s, \quad (\rho_i = a_i) \tag{18}$$

2.4. Scattering Cross Section

In order to solve unknown expansion coefficients, it is necessary to express the scattering field from other cylinders to local coordinate of the i-th cylinder. By using the addition theorem, the transformation from the l-th to i-th coordinates:

$$H_m^{(2)}(k\rho_l)e^{jm\varphi_l} = \sum_{n=-\infty}^{\infty}J_n(k\rho_i)H_{n-m}^{(2)}(kd_{il})e^{jn\varphi_i}e^{-j(n-m)\varphi_{il}} \quad \text{for} \quad \rho_l < d_{il}. \tag{19}$$

The boundary condition can be written in the following matrix form

$$\begin{bmatrix} M_{1H} & M_{2H} \\ M_{1E} & M_{2E} \end{bmatrix}\begin{bmatrix} B \\ C \end{bmatrix} = \begin{bmatrix} H_z^{inc} \\ E_z^{inc} \end{bmatrix} \tag{20}$$

where vectors $\mathbf{B}$, $\mathbf{C}$, $\mathbf{H_z^{inc}}$, and $\mathbf{E_z^{inc}}$ represent coefficients B_{lm}, C_{im}, the incident magnetic and electric fields, respectively. All vectors have the size of $(2\mathrm{N}+1)\mathrm{M}$, where M is the number of cylinders, and N is a number which should be large enough for convergence. The infinite series of Bessel function are rapidly convergent for a small-size anisotropic cylinder, and the number N which satisfies the relation $N = 3(ka_i + 1)$ is sufficient to obtain reasonable accuracy. On the other hand, for very large dimensions or large values of the medium parameters, one may need a large number of terms to achieve the convergence of Bessel functions. However, large errors or singular matrices may occur in evaluating the inverse matrix in Eq. (20), so the electrical dimensions in our numerical calculations are restricted within the range of a small or medium size.

The elements of $\mathbf{M_{1H}}$, $\mathbf{M_{2H}}$, $\mathbf{M_{1E}}$ and $\mathbf{M_{2E}}$ are given by

$$M_{1H}(i_x,j_x) = \begin{cases} -j^{n-m}J_n(ka_i)H_{n-m}^{(2)}(kd_{il})\exp(-j(n-m)\varphi_{il}), & i \neq l \\ -H_n^{(2)}(ka_i)\delta_{i_xj_x}, & i = l \end{cases} \tag{21}$$

$$M_{2H}(i_x,j_x) = \begin{cases} H_{nm}(a_i), & i = l \\ 0, & i \neq l \end{cases} \tag{22}$$

$$M_{1E}(i_x,j_x) = \begin{cases} -j^{n-m+1}\sqrt{\frac{\mu_0}{\varepsilon_0}}J'_n(ka_i)H_{n-m}^{(2)}(kd_{il})\exp(-j(n-m)\varphi_{il}), & i \neq l \\ -j\sqrt{\frac{\mu_0}{\varepsilon_0}}H'^{(2)}_n(ka_i)\delta_{i_xj_x}, & i = l \end{cases} \tag{23}$$

$$M_{2E}(i_x,j_x) = \begin{cases} E_{nm}(a_i), & i = l \\ 0, & i \neq l \end{cases} \tag{24}$$

where n, $m = 0, \pm1, \pm2, \ldots \pm N$, and $i, l = 0, 1, \ldots, M$. The elements of $\mathbf{H_z^{inc}}$ and $\mathbf{E_z^{inc}}$ are given by

$$H_z^{inc}(i_x) = A_n e^{jk\rho_i'\cos(\varphi_i'+\varphi_0)}J_n(ka_i)e^{jn\varphi_0} \tag{25}$$

$$E_z^{inc}(i_x) = j\sqrt{\frac{\mu_0}{\varepsilon_0}}A_n e^{jk\rho_i'\cos(\varphi_i'+\varphi_0)}J_n'(ka_i)e^{jn\varphi_0} \tag{26}$$

The scattering cross section of the multiple homogeneous anisotropic cylinders is given by:

$$\frac{\sigma}{\lambda}(\varphi,\varphi_0)=\frac{2}{\pi}\left|\sum_{l=1}^{M}\sum_{m=-N}^{N}B_{lm}e^{jk\rho_l'\cos(\varphi_l'-\varphi)}e^{jm\varphi}\right|^2 \tag{27}$$

3. NUMERICAL RESULTS

To check the validity and accuracy of the proposed method and associated code, the far scattered field pattern from a homogeneous anisotropic cylinder due to an incident TE plane wave with $\varphi_0 = 180^{\circ}$ is shown in Fig. 2. The radius of the cylinder is equal to 0.25λ, and the electromagnetic parameters are $\varepsilon_{xx} = 4\varepsilon_{yy} = 4\varepsilon_0$, $\varepsilon_{xy} = \varepsilon_{yx} = 0$, $N = 8$, and $\mu_{zz} = 2\mu_0$. It is obvious that the two patterns are in good agreement, which indicates the validity of this method in modeling homogeneous anisotropic objects by small circular cylinders.

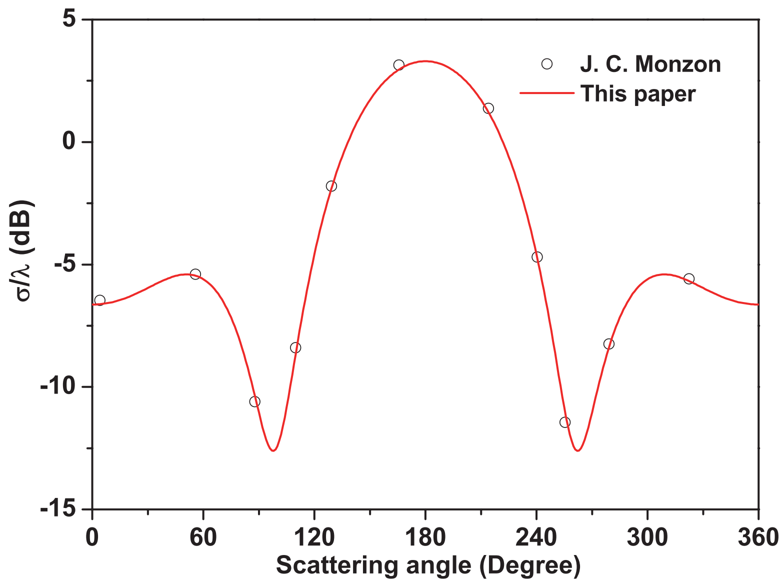

Figure 2. The scattering cross section of a homogeneous anisotropic cylinder for TE polarized. The markers are the solution taken from Ref. [9] [Fig. (3a)].

Figure 3 shows the effects of different numbers of scatters on the radar cross section (RCS) when the size of cylinders remains unchanged. The parameters are $a_0\lambda = 0.3$, $b_0\lambda = 0.2$, $\rho_0/\lambda = 10.0$, $a_i = 0.1\lambda$, $N = 5$, $\varphi_0 = 180^{\circ}$, $\varepsilon_{x_ix_i} = 4\varepsilon_{y_iy_i} = 4\varepsilon_0$, $\varepsilon_{x_iy_i} = \varepsilon_{y_ix_i} = 0$, and $\mu_{z_iz_i} = 2\mu_0$. The forward-scattering cross section is significantly affected by the number of scatters because the cylinders act as convex lens.

Figure 4 shows the scattering cross section of three homogeneous anisotropic cylinders with different sizes. Three cylinders are located on the y-axis located at $(0, -0.5\lambda)$, $(0, 0)$, and $(0, 0.5\lambda)$. The other parameters are $a_0\lambda = 0.3$, $b_0\lambda = 0.2$, $\rho_0/\lambda = 10.0$, $\varphi_0 = 180^{\circ}$, $N = 3(ka_i+1)$, $\varepsilon_{x_ix_i} = 2.5\varepsilon_0$, $\varepsilon_{y_iy_i} = 1.5\varepsilon_0$, $\varepsilon_{x_iy_i} = \varepsilon_{y_ix_i} = 0$, and $\mu_{z_iz_i} = 2\mu_0$. As one can see from this figure, RCS is symmetrical around 180° due to the symmetry of three cylinders. The peak value of forward scattering cross section increases with the size of scatters.

Figure 5 shows the scattering cross section of three homogeneous anisotropic cylinders with different beamwidth of Gaussian beam. Three cylinders with 0.2λ radius are located at $(-0.5\lambda, 0)$, $(0, 0)$, and $(0.5\lambda, 0)$. The other parameters are $\varphi_0 = 180^{\circ}$, $N = 7$, $\varepsilon_{x_ix_i} = 2.5\varepsilon_0$, $\varepsilon_{y_iy_i} = 1.5\varepsilon_0$, $\varepsilon_{x_iy_i} = \varepsilon_{y_ix_i} = \varepsilon_0$, and $\mu_{z_iz_i} = 2\mu_0$. Figure 6 shows the scattering cross section of three homogeneous anisotropic cylinders with different anisotropic materials. The parameters are $a_0\lambda = 0.3$, $b_0\lambda = 0.2$, $\rho_0/\lambda = 10.0$, $\varphi_0 = 180^{\circ}$, $a_i = 0.2\lambda$, $N = 7$, $\varepsilon_{y_iy_i} = \varepsilon_0$, $\varepsilon_{x_iy_i} = \varepsilon_{y_ix_i} = 0$, and $\mu_{z_iz_i} = 2\mu_0$. As can be seen from these two figures, the effect of Gaussian beam and anisotropic materials on the scattering cross section is slight for the given parameters.

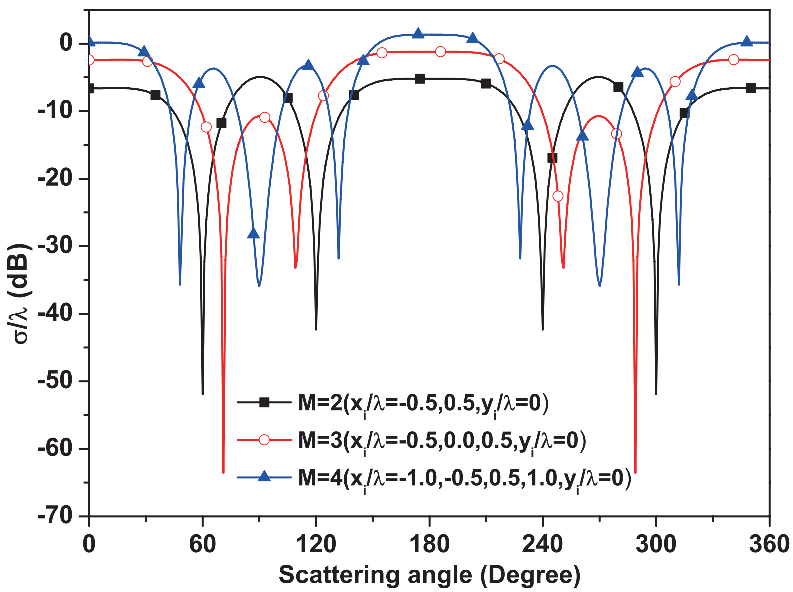

Figure 3. The Gaussian beam scattering cross section for TE polarized of different numbers of homogeneous anisotropic cylinders.

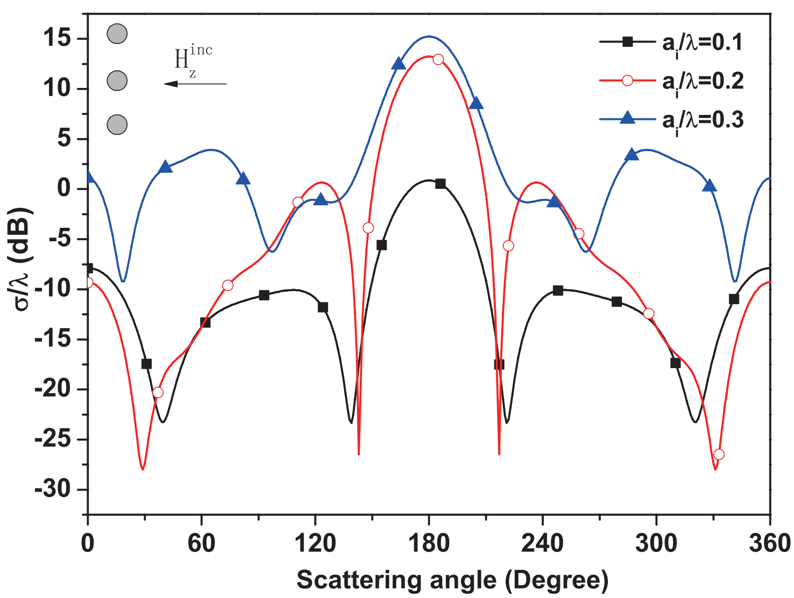

Figure 4. The Gaussian beam scattering cross section for TE polarized of homogeneous anisotropic cylinders with different sizes.

The near-field distribution is computed when cylinders is illuminated by a Gaussian beam at an angle of 180° in Figs. 7–8. Fig. 7 shows the z-component of magnetic field for two homogeneous anisotropic cylinders. Two cylinders are located at $(0, -0.5\lambda)$ and $(0, 0.5\lambda)$. The other parameters are $a_0\lambda = 0.3$, $b_0\lambda = 0.2$, $\rho_0/\lambda = 10.0$, $\varphi_0 = 180°$, $a_i = 0.1\lambda$, $N = 5$, $\varepsilon_{x_ix_i} = 2\varepsilon_{y_iy_i} = 4\varepsilon_0$, $\varepsilon_{x_iy_i} = \varepsilon_{y_ix_i} = 0$, and $\mu_{z_iz_i} = 2\mu_0$. Fig. 8 shows the near-field for four homogeneous anisotropic cylinders with the same geometry. Four cylinders are located at $(0, -0.5\lambda)$, $(-0.5\lambda, 0)$, $(0, 0.5\lambda)$, and $(0.5\lambda, 0)$. The parameters are the same as those in Fig. 7 except for $\varepsilon_{y_iy_i} = \varepsilon_0$.

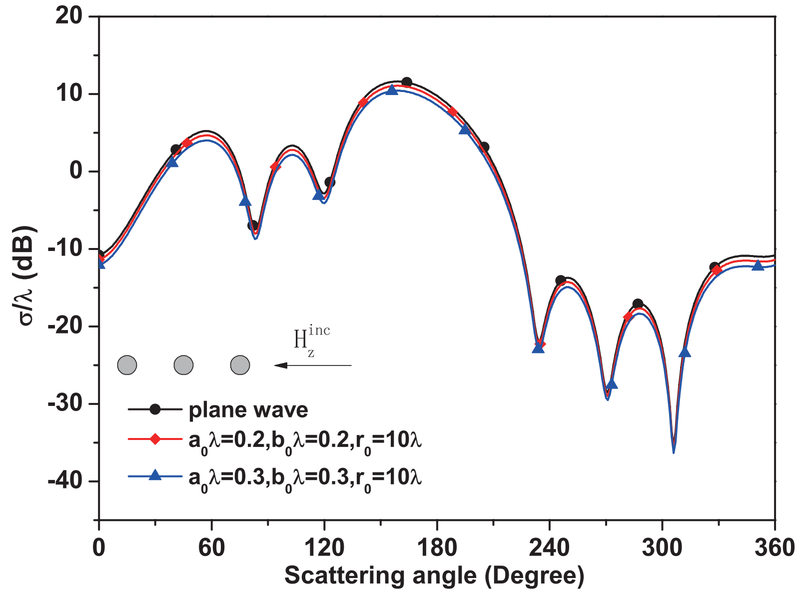

Figure 5. The scattering cross section for TE polarized of three homogeneous anisotropic cylinders with different beam width of Gaussian beam.

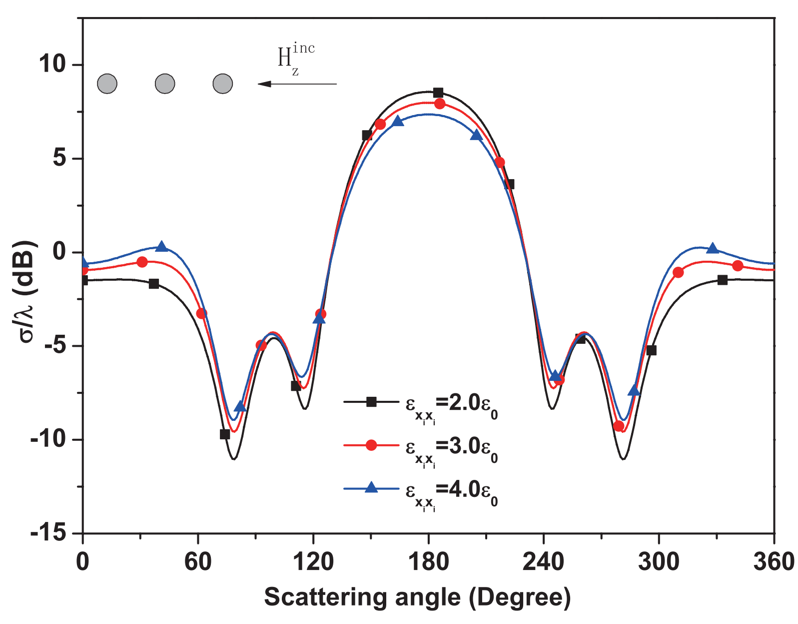

Figure 6. The Gaussian beam scattering cross section for TE polarized of three homogeneous anisotropic cylinders with different anisotropic materials.

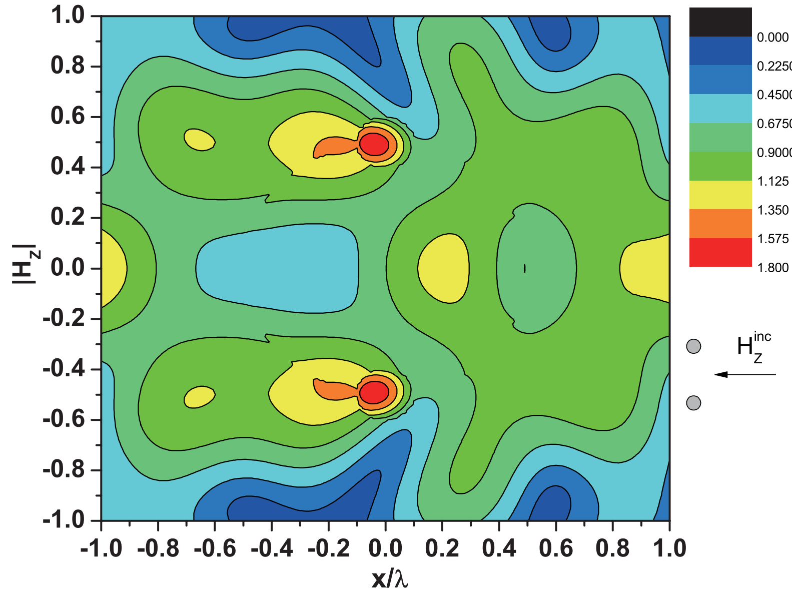

Figure 7. The near magnetic field for two homogeneous anisotropic cylinders.

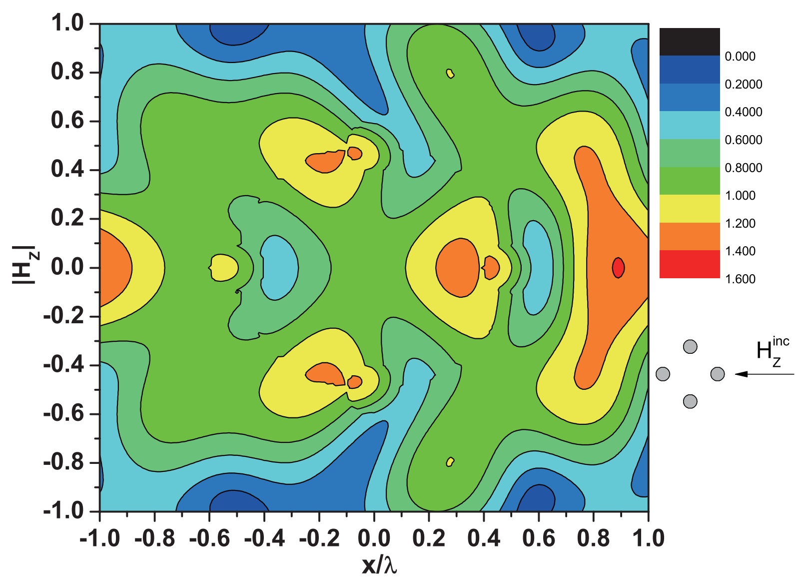

Figure 8. The near magnetic field for four homogeneous anisotropic cylinders.

4. CONCLUSION

A formulation for multiple scattering of a Gaussian beam wave from an array of parallel homogeneous anisotropic cylinders has been derived. The analysis is based on the boundary value approach, which leads to a matrix equation of an infinite size. The matrix is truncated to the order that assumes numerical convergence. Scattering cross sections and near fields behavior of an array of parallel homogeneous anisotropic cylinders have been discussed and analyzed, which are of useful values for the development of approximate and numerical techniques as well as antennas and radar applications.

ACKNOWLEDGMENT

This work was supported by the National Natural Science Foundation of China [Grant number 62171355]; Sci. & Tech. Program of Suqian [Grant number K202017].

REFERENCES

1. Mizrahi, E. and T. Melamed, "Plane wave scattering by a moving PEC circular cylinder," *IEEE Transactions on Antennas and Propagation*, Vol. 66, 3623–3630, 2018.
2. Dikmen, F., E. Sever, S. Vatansever, and Y. A. Tuchkin, "Well-conditioned algorithm for scattering by a few eccentrically multilayered dielectric circular cylinders," *Radio Science*, Vol. 50, 99–110, 2015.
3. Montaseri, N., A. Abdolali, M. Soleimani, and V. Nayyeri, "Plane wave scattering by a circular PEMC cylinder coated with anisotropic media," *International Journal of RF and Microwave Computer-Aided Engineering*, Vol. 23, 225–231, 2012.
4. Yang, J., L.-W. Li, K. Yasumoto, and C.-H. Liang, "Two-dimensional scattering of a gaussian beam by a periodic array of circular cylinders," *IEEE Transactions on Geoscience and Remote Sensing*, Vol. 43, 280–285, 2005.
5. Kushta, T. and K. Yasumoto, "Electromagnetic scattering from periodic arrays of two circular cylinders per unit cell," *Progress In Electromagnetics Research*, Vol. 29, 69–85, 2000.
6. Elsherbeni, A. Z. and A. A. Kishk, "Modeling of cylindrical objects by circular dielectric and conducting cylinders," *IEEE Transactions on Antennas and Propagation*, Vol. 40, 96–99, 1992.
7. Yokota, M., T. Takenaka, and O. Fukumitsu, "Scattering of a Hermite-Gaussian beam mode by parallel dielectric circular cylinders," *Journal of the Optical Society of America A*, Vol. 3, 580–586, 1986.
8. Shooshtari, A. and A. R. Sebak, "Electromagnetic scattering by parallel metamaterial cylinders," *Progress In Electromagnetics Research*, Vol. 57, 165–177, 2006.
9. Monzon, J. C. and N. J. Damaskos, "Two-dimensional scattering by a homogeneous anisotropic rod," *IEEE Transactions on Antennas and Propagation*, Vol. 34, 1243–1249, 1986.
10. Kozaki, S., "A new expression for the scattering of a Gaussian beam by a conducting cylinder," *IEEE Transactions on Antennas and Propagation*, Vol. 30, 881–887, 1982.